

A Coupled Fluid-Structure Analysis for 3D Flutter in Turbomachines

Vitaly GNESIN,

Department of Aerohydromechanics, Institute for Problems in Machinery Ukrainian National Academy of Sciences,
2/10 Pozharsky st., Kharkov 310046, UKRAINE

Romuald RZĄDKOWSKI

Institute of Fluid-Flow Machinery, Polish Academy of Sciences,
Fiszera 14, PL 80-952 Gdańsk, Poland,
Polish Naval Academy, Faculty of Mechanical and Electrical Engineering

Luba KOLODYAZHNAYA

Department of Aerohydromechanics, Institute for Problems in Machinery Ukrainian National Academy of Sciences,
2/10 Pozharsky st., Kharkov 310046, UKRAINE

ABSTRACT

A three-dimensional nonlinear time-marching method and numerical analysis for aeroelastic behaviour of oscillating blade row has been presented. The approach is based on the solution of the coupled fluid-structure problem in which the aerodynamic and structural equations are integrated simultaneously in time. In this formulation of a coupled problem, the interblade phase angle at which a stability (or instability) would occur, is a part of the solution. The ideal gas flow through multiple interblade passage (with periodicity on the whole annulus) is described by the unsteady Euler equations in the form of conservative laws, which are integrated by use of the explicit monotonous second order accurate Godunov-Kolgan volume scheme and a moving hybrid H-H (or H-O) grid. The structure analysis uses the modal approach and 3D finite element model of the blade. The blade motion is assumed to be a linear combination of modes shapes with the modal coefficients depending on time. The influence of the natural frequencies on the aerodynamic coefficient and aeroelastic coupled oscillations for the Fourth Standard Configuration is shown. The stability (instability) areas for the modes are obtained. It has been shown that interaction between modes plays an important role in the aeroelastic blade response. This interaction has essentially nonlinear character and leads to blade limit cycle oscillations.

NOMENCLATURE

IBPA	- interblade phase angle [deg.],
H	-source vector,
p	- pressure, [MPa],
t	- temperature, [°C],
δ	- interblade phase angle [deg.],
ε	- internal energy of mass unit,
χ	- ratio of the fluid specific heats,
Ω	- finite volume.

INTRODUCTION

Modern turbomachines operate under very complex regimes where a mixture of subsonic, transonic and supersonic regions coexist. With recent advances in internal compressible flow modelling and increased computational power, it is now possible to undertake both steady and unsteady flow analysis of very complex turbomachinery geometry. The trend for improved gas turbine engine design with higher aerodynamic blade loading and smaller physical size attracts much attention to the aeroelastic behaviour of blades not only in compressors, but also in turbines. Flow-induced blades oscillations of the turbine and compressor can lead to fatigue failures of a construction and so they represent an important problem of reliability, safety, and operating cost.

Aeroelasticity phenomena are characterised by the interaction of fluid and structural domains, most prediction methods tend to treat the two domains separately, and they usually assume some critical interblade phase angle for which the flutter analysis is carried out for a single passage.

The undeniable importance of spatial and nonlinear effects for practical turbomachinery configurations has led to the development of three - dimensional methods. Since the early 1980's a number of time accurate Euler and Navier - Stokes procedures have been developed to predict blade row unsteady flows in which unsteadiness is caused by aerodynamic disturbances at the inflow or outflow boundaries, relative motions between the blade rows, or blade vibrations. The traditional approach in flutter calculations of bladed disks is based on frequency domain analysis (Bölcs and Fransson, 1986, Moyroud, F., Jacquet – Richardet, G., and Fransson, T., H., 1996), in which the blade motions are assumed to be harmonic functions of time with a constant phase lag between adjacent blades, and the mode shapes and frequencies are obtained from structural computations. This approach ignores the feedback effect of the fluid on the structural vibration.

In recent times, the new approaches based on the simultaneous integration in time of the equations of motion for the structure and the fluid have been developed (Bakhle et al. 1992, He, 1994; Bendiksen, 1998; Rządowski et al., 1997, Gnesin 1999). These approaches are very attractive due to the general formulation of a coupled problem, as the interblade phase angle at which a stability (instability) would occur is a part of solution.

In the present study the simultaneous time integration method has been described to calculate the aeroelastic behaviour for a three-dimensional oscillating blade row in transonic gas flow.

AERODYNAMIC MODEL

The flow model is described in detail in (Sokolovsky and Gnesin, 1986; Gnesin and Kolodyazhnaya, 1999), a brief summary will be given here for the sake of completeness. It is considered the 3D transonic flow of an ideal gas through a multipassage blade row. In the general case the flow is assumed to be a periodic function from blade to blade (in pitchwise direction), so the calculated domain includes all blades of the whole assembly (Fig. 1).

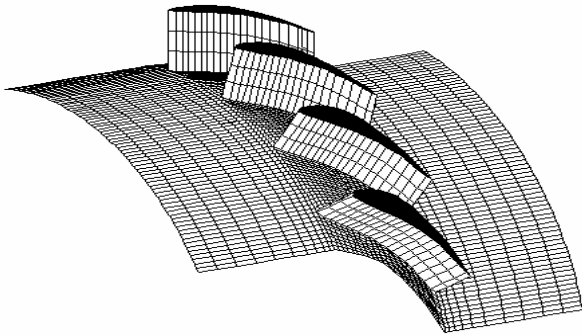


Figure 1. A view of a sector of the whole blade assembly

The flow equations will be written for a three dimensional Cartesian coordinate system which is fixed to a rotating blade row. In this case, the conservative form of the unsteady Euler equations is given (Gnesin and Kolodyazhnaya, 1999):

$$\frac{\partial}{\partial t} \int_{\Omega} f d\Omega + \oint_{\sigma} \vec{F} \cdot \vec{n} d\sigma + \int_{\Omega} H d\Omega = 0. \quad (1)$$

Here f is the solution vector; \vec{F} is the inviscid flux through the lateral area σ bounding the finite volume Ω , and H is source vector which contains the terms due to the rotation of the coordinate system. The above system of equations is completed by the perfect gas equation

$$p = \rho \varepsilon (\chi - 1), \quad (2)$$

where χ denotes the ratio of the fluid specific heats ε is an internal energy of mass unit. The spatial solution domain is discretized using linear hexahedral elements. The equations (1–2) are integrated on moving H-H (or H-O) – type grid with use of explicit monotonous second – order accuracy Godunov – Kolgan difference scheme (Sokolovsky and Gnesin, 1986).

We assume that the unsteady fluctuations in the flow are due to prescribed blade motions, and the flows far upstream and far downstream from the blade row are at most small perturbations of uniform free streams. So the boundary conditions formulation is based on one – dimensional theory of characteristics, where the number of physical boundary conditions depends on the number of characteristics entering the computational domain.

In the general case, when axial velocity is subsonic, at the inlet boundary initial values for total pressure, total temperature and flow angles are used in terms of the rotating frame of reference, while at the outlet boundary only static pressure has to be imposed. On the blade surface, zero flux is applied across the solid surface (the grid moves with the blade).

In general, computations are made using a number of blades passages equal to the number of blades in the cascade. Periodic conditions are applied at the upper and lower boundaries of the calculated domain at each time moment. However there are some situations where it is possible to reduce the number of passages used in the calculations. For unsteady flows in which all blades perform harmonic oscillations with the particular mode shape, frequency and a constant interblade phase angle (IBPA) (tuned cascades), the number of blades passages depends on the value of the interblade phase angle. For instance, computations with the phase angle $\delta = \pm 90$ deg. can be made for four passages. In the time domain method, in which the motion of the blades of a coupled fluid-structure problem is not known in advance, it is necessary in the numerical calculations include all blade passages. The time step at the coupled calculations is assumed to be constant and is chosen from the stability conditions of the explicit scheme for the fluid model.

STRUCTURAL MODEL

The structural model is based on a linear modal model (Rządowski 1998), the mode shapes and natural frequencies being obtained via standard FE analysis techniques. Each blade is treated as an individual during the numerical calculations.

The structural part of the aeroelastic equations of motion are uncoupled by using the mode shape matrix. Boundary conditions from the structural and aerodynamic domains are exchanged at each time step and the aerodynamic mesh is moved to follow the structure motion (the partially coupled method). The structural damping is not included here. The scheme used to integrate the structural equations is the same as the scheme used in the flow code. For this scheme the accuracy of the calculations of natural frequencies and mode shapes is sufficient. The integration scheme introduce a damping; this value is very small and was found from calculations done with the aerodynamic forces set to zero.

NUMERICAL RESULTS

The numerical calculations have been carried out for the turbine cascade known as the Fourth Standard Configuration, which has been experimentally investigated in the nonrotating annular cascade tunnel in transonic flow (Bölcs and Fransson, 1986). As the first step the numerical calculations were performed to compare with the experimental ones.

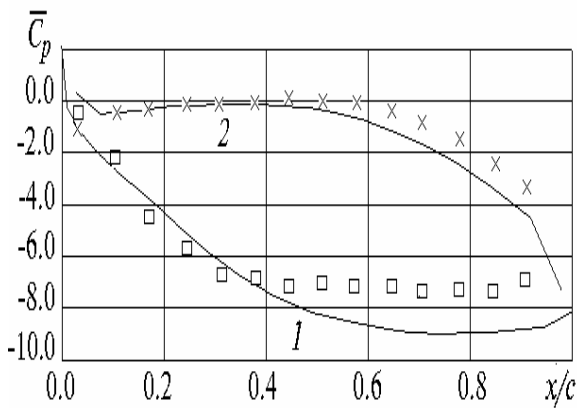


Figure 2a. The time averaged pressure coefficient distribution over the blade chord (1 suction side, 2 pressure side, \square \square pressure side experiment, \times \times suction side experiment)

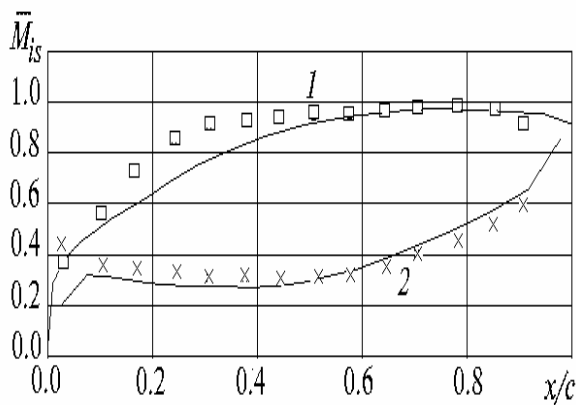


Figure 2b. The Mach number (b) distribution over the blade chord (1 suction side, 2 pressure side, \square \square pressure side experiment, \times \times suction side experiment)

The steady and unsteady predictions have been made on the hybrid H-H type grid with $10 \times 30 \times 60$ grid points including moving H-grid (16 points across) near the blade. In order to compare the results for the unsteady flow, the numerical results for the steady flow must be validated, because they are the starting point for the unsteady flow calculations. In Fig 2a. the calculated and experimental results of steady pressure coefficient are presented and in Fig 2 b the distribution of the isentropic Mach number along the middle section of the blade is shown. The integers "1" and "2" corresponds to the suction and pressure sides respectively. Agreement between the numerical and experimental results is quite good. The small discrepancies are noticeable near the leading edge at approximately 30% of the chord length on the suction side.

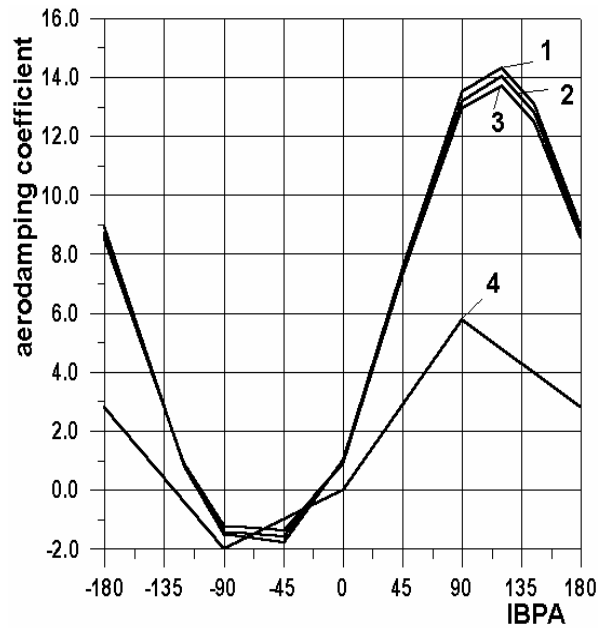


Figure 3. Aerodamping coefficient in dependence of interblade phase angle (1 – casing, 2 – mid , 3 – hub, 4 experiment)

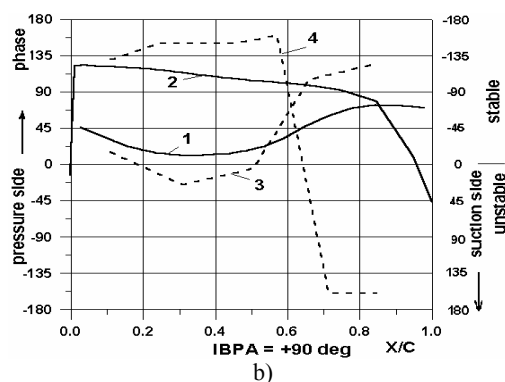
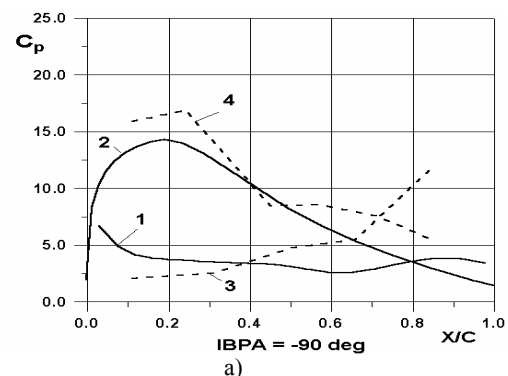
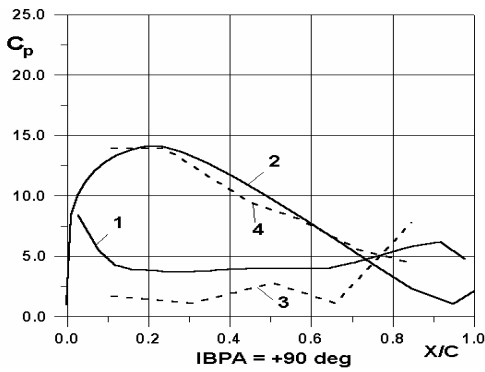
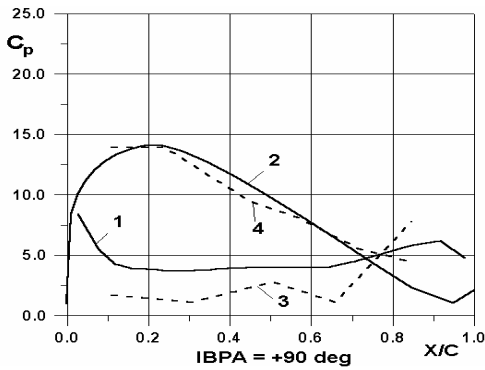


Figure 4a. The first harmonic unsteady pressure amplitude (a, b) along the blade chord (1 pressure side theory, 2 suction side theory, 3 pressure side experiment, 4 suction side experiment)



c)

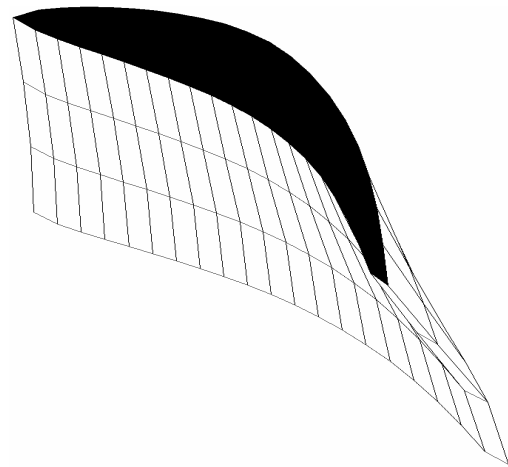


d)

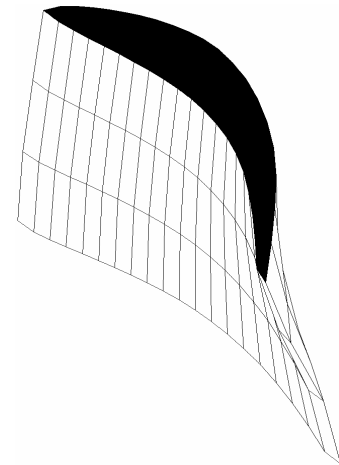
Figure 4b. The phase (c, d) distribution along the blade chord (1 pressure side theory, 2 suction side theory, 3 pressure side experiment, 4 suction side experiment)

The influence of the interblade phase angle on the aerodamping coefficient for the assumed bending oscillations has been shown in Fig 3. Aerodamping coefficient D is equal to the negative work coefficient during one cycle of oscillations. In that figure the numerical calculated aerodamping coefficients in the hub ("1"), middle ("2") and root ("3") sections and the experimental ones ("4") are presented. From these results the strong influence of IBPA is visible. In the range of $-120 \text{ deg.} < \text{IBPA} < -30 \text{ deg.}$ the aerodamping coefficients have negative values, that corresponds to the transfer of energy from the flow to the oscillating blades. The maximum aerodamping coefficient is for IBPA close to 90 deg. In this case the aerodamping coefficient does not depend on the blade length. The experimental values of the aerodamping coefficient is close to the calculated results although the small difference is found in the vicinity of the maximum value of the aerodamping coefficient.

The comparison of the calculated and experimental distribution of the first harmonic amplitude and phase for IBPA of $\pm 90 \text{ deg.}$ is presented in Fig 4. The agreement is satisfactory. The minimal and maximal values of unsteady pressure occur for in-phase and counter-phase oscillations respectively. The energy exchange between the passing flow and the vibrating blade is defined by the pressure phase shift relatively to the blade motion. The positive phase shift on the pressure side and the negative phase shift on the suction side correspond to aerodamping of the system (stability).



1st mode shape



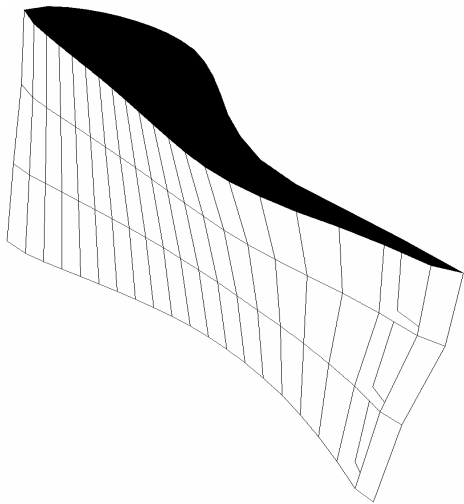
2nd mode shape

Figure 5. The natural mode shapes of the blade

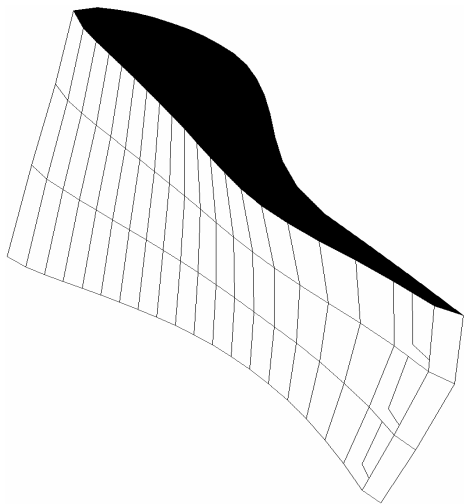
In the next step of the numerical study the influence of the first four mode shapes on the blade response in the coupled fluid-structure calculations is shown. The mode shapes of the considered blade are presented in Fig 5. The first mode is mainly the bending mode, the second one is the torsional mode, the third and fourth ones are the bending-torsion modes. The natural frequencies are equal to the 150 Hz, 750 Hz, 900 Hz and 1050 Hz respectively.

Figures 6 and 7 show the aerodamping coefficient versus the interblade phase angle for the first and second natural mode shapes of STC4 respectively under harmonic oscillations with different frequencies (calculated by 3D flutter aerodynamic model). The

negative values of Ψ correspond to the transfer of energy from the flow to the blade (self-excitation), and the positive values - to dissipation of an oscillating blade energy to the flow. All curves have the typical sinusoidal forms. It is seen that the aerodamping grows as the oscillation frequency increases.



3rd mode shape



4th mode shape

Figure 5. The natural mode shapes of the blade

It should be pointed out that the oscillations according to the first mode (bending oscillations) are characterised by the negative values of aerodamping coefficient near the IBPA of -90 deg. (see Fig.6), while the oscillations according to the second mode have the self-excitation area near the IBPA of 90 deg. (see Fig.7).

1st MODE SHAPE

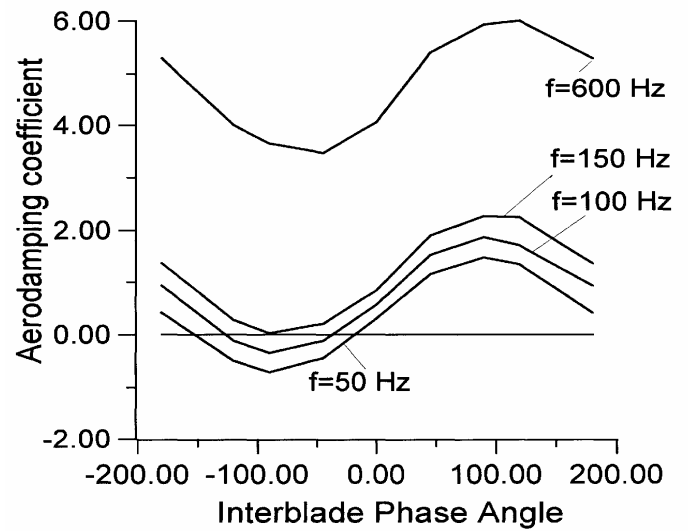


Figure 6. Aerodamping coefficient versus interblade phase angle for the 1st mode of vibration and different vibration frequencies

2nd MODE SHAPE

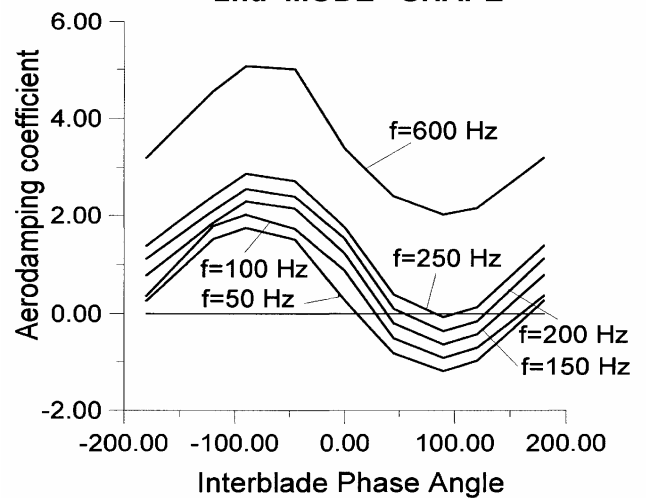


Figure 7. Aerodamping coefficient versus interblade phase angle for the 2nd mode of vibration and different vibration frequencies

The influence of the phase angle on the sign of the aerodamping coefficient is important for the low modes of vibration and low natural frequencies. It decreases with increasing of the mode number and natural frequencies. Aerodamping coefficient grows almost linearly taking positive values over all frequency range except the area of low frequencies ($f < 300$ Hz). Fig. 8 shows the areas of

possible instability for STC4 (IV Standard Configuration). It can be seen that instability of the first mode appears at the phase angle equal to -90 deg. ($f < 150$ Hz) whereas the instability of the second mode appears at phase angle equal to $+90$ deg. ($f < 250$ Hz). The higher the natural modes are the more stable the cascade is, over the full frequency range.

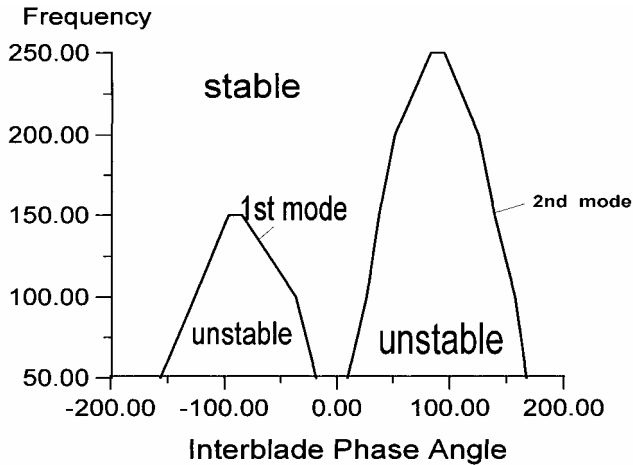


Figure 8. The stability regions for the 1st and 2nd mode shapes

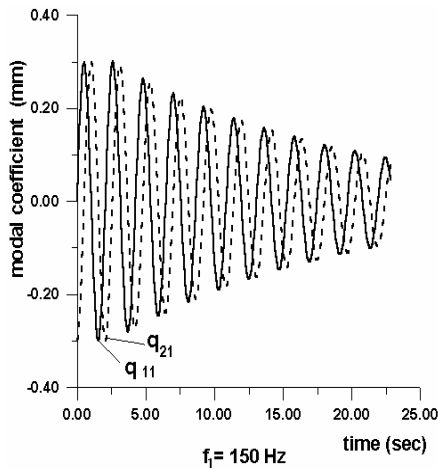


Figure 9. The aeroelastic oscillations of two adjacent blades for the first mode

The sign of the aerodamping coefficient calculated for the harmonic oscillations, may be considered only as a necessary but not sufficient condition for self-excited oscillations. The final estimation of the blade row aeroelastic behaviour may be obtained on the basis of the coupled fluid-structure solution in the time marching algorithm. In this case the blade response is defined not only by the harmonic time history, at which the aerodamping coefficient has been calculated, but

also by such parameters which influence the aerodynamic force as the mass flow, the blade mass and the natural frequency of the blade.

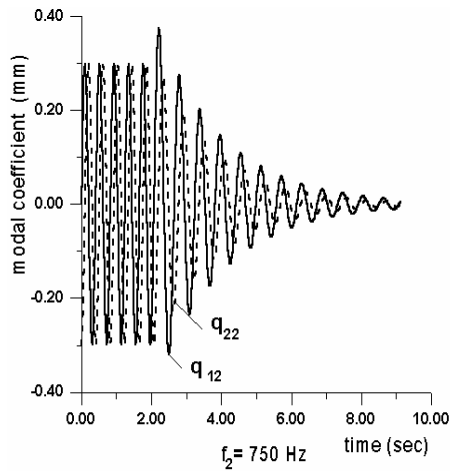


Figure 10. The aeroelastic oscillations of two adjacent blades corresponding to the second mode

All calculations were run from the very beginning for harmonic oscillations until the steady state periodic flow through vibrating blade row is converged. During this time the forced frequencies of harmonic oscillations of each mode were equal to their natural frequencies respectively. After some time moment, named as the start regime, there began the coupled vibrations in which the blade displacements and velocities, and the flow parameters are used as the initial conditions for the coupled time-integration procedure. Let us consider the aeroelastic blade response, vibrating from the beginning at the harmonic oscillations with IBPA of -90 deg., and next according to fluid-structure interaction.

Figure 9 illustrates the two adjacent blades motion of the first mode with forced frequency 150 Hz. It corresponds to aerodamping coefficient value close to zero (see Fig. 6). Here q_{11} and q_{21} denote the modal coefficients for the first and second blade oscillating of the 1st mode. As it has seen from Fig. 9 the blade oscillations are damped with the logarithmic decrement equal to approximately constant value. It indicates that the blade motion is close to the linear damped oscillations

Figure 10 presents the analogous graphs for the two adjacent blades oscillations corresponding to the 2nd mode of vibration, Figure 11 to the 3rd mode and Figure 12 to the 4th mode. For all regimes the oscillations are damped. The higher the natural frequency the more stable the blade is.

The different character of blade motion was observed for consideration of the interaction of the natural mode vibrations. Figure 13 shows the blade response at the harmonic oscillations corresponding to the first and second modes. It is clearly observed that response of the blade for the 2nd mode shape decays, but the amplitude of the 1st mode tends to the approximately constant value, that corresponds to the limit cycle of oscillations. The similar situation is observed for harmonic oscillation corresponding to first up to fourth

natural modes. Figure 14 shows the blade response for taking into account the interaction of different natural modes at the initial IBPA of + 90deg. Although the aerodamping coefficient at the harmonic oscillation is positive (that corresponds to the stable motion), the transient behaviour is observed and the blades motion changes to the oscillations with a interblade phase angle equal to - 90 deg.

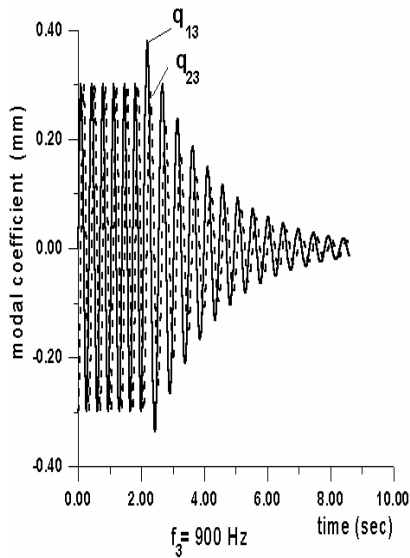


Figure 11. The aeroelastic oscillations of two adjacent blades corresponding to the third mode

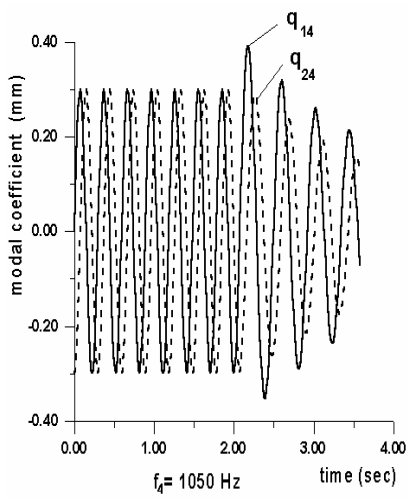


Figure 12. The aeroelastic oscillations of two adjacent blades corresponding to the fourth mode

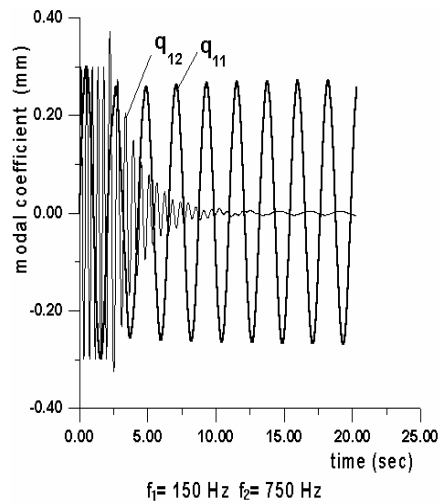


Figure 13 The aeroelastic oscillations of two adjacent blades corresponding to the 1st and 2nd mode

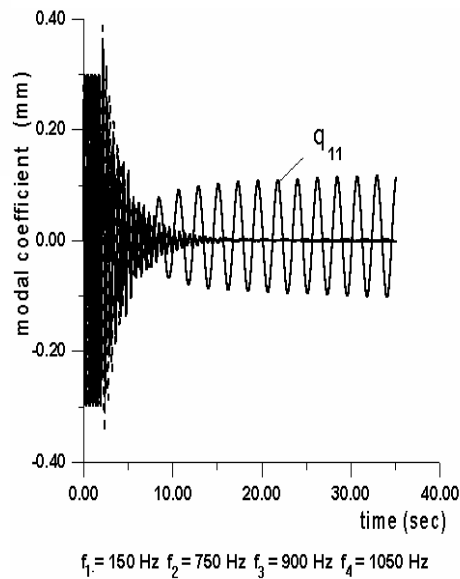


Figure 14. The blade oscillations by the 1st, 2nd, 3d and 4th modes (IBPA of +90 deg.)

As IBPA of -90 deg. represents an unstable condition for the first mode, the amplitude of the first mode grows approaching to the limit cycle of oscillations.

CONCLUSIONS

In the present study, the simultaneous time domain method and the modal superposition method is used to determine the aeroelastic stability of the cascade. The numerical analysis of the influence of the natural modes on an aeroelastic blade response for 4th Standard Configuration has been carried out. It has shown that each of mode shapes oscillations in the range of frequencies $f > 150$ Hz is damped. The interaction between the modes shapes has essentially nonlinear character and leads to limit cycle vibrations (blade auto - oscillations).

The presented time domain method allows a more realistic simulation of the motion of the fluid and the cascade blades that should lead to a better physical understanding.

REFERENCES

- Bakhle, M.A., Reddy, T.S.R., and Keith T.G., 1992, "Time Domain Flutter Analysis of Cascades Using a Full-Potential Solver", AIAA J. vol.30, No 1, p.163.
- Bendiksen, O., O., 1998, "Nonlinear Blade Vibration and Flutter in Transonic Rotors", Proc. of ISROMAC - 7, The 7th Intern. Symp. on Transport Phenomena and Dynamics of Rotating Machinery, Feb., 22-26, 1998. Honolulu, Hawaii, USA, p. 664.
- Böls, A., and Fransson, T.H., 1986, "Aeroelasticity in Turbomachines: Comparison of Theoretical and Experimental Cascade Results", Communication du LTAT. - EPFL Switzerland, No 13, p. 174.
- He L., 1984, "Integration of 2D Fluid / Structure Coupled Systems for Calculation of Turbomachinery Aerodynamic, Aeroelastic Instabilities", J. of Computational Fluid Dynamics. vol.3, p.217.
- Gnesin, V., I., and Kolodyazhnaya, L., V., 1999, "Numerical Modelling of Aeroelastic Behaviour for Oscillating Turbine Blade Row in 3D Transonic Ideal Flow", Problems in Machinery Engineering, vol. 1, No 2, p. 65-76.
- Gnesin, V.I., 1999, "A Numerical Study of 3D Flutter in Turbomachines using a Fluid Structure Coupled Method", Engineering Mechanics, Vol. 6, No 4/5, 253-267
- Moyroud, F., Jacquet - Richardet, G., and Fransson, T., H., 1996, "A Modal Coupling for Fluid and Structure Analysis of Turbomachine Flutter Application to a Fan Stage", ASME Paper 96 - GT - 335, p.1-19.
- Rządowski, R., 1998, "Dynamics of Steam Turbine Blading, Part Two Bladed Discs", Ossolineum, Wrocław-Warszawa.
- Rządowski, R., Gnesin, V. and Kovalov, A., 1997, "The 2D Flutter of Bladed Disc in an Incompressible Flow", The 8th International Symposium of Unsteady Aerodynamics and Aeroelasticity of Turbomachines, Stockholm, Sweden, Sept. 14-18, p.317-334.
- Sokolovsky, G., A., and Gnesin V.,I., 1986, "Unsteady and Viscous Flows in Turbomachines", Naukova Dumka, Kiev (in Russian).